FEMTOSECOND FIBER TIMING DISTRIBUTION SYSTEM FOR THE LINAC COHERENT LIGHT SOURCE*

Heng Li[1,3,4], Li-Jin Chen[5], Haynes Pak Hay Cheng[5], Justin E. May[4],Steve Smith[4], Kerstin Muehlig[4], Akshaya Uttamadoss[4,6], Josef C. Frisch[4], Alan R. Fry[4], Franz X. Kärtner[7,8], Philip H. Bucksbaum[1,2,3,4]

[1] Stanford PULSE Institute, [2] Department of Physics, and [3] Department of Applied Physics, Stanford University, Stanford, CA, USA
[4] SLAC National Accelerator Laboratory, Menlo Park, CA, USA
[5] Idesta Quantum Electronics, LLC, Newton, NJ, USA
[6] Department of Electrical Engineering, Princeton University, Princeton, NJ, USA
[7] Department of Electrical Engineering and Computer Science, and Research Laboratory of Electronics, Massachusetts Institute of Technology, Cambridge, MA, USA
[8] Center for Free-Electron Laser Science, DESY, and Physics Department, University of Hamburg, Hamburg, Germany

Abstract

We present the design and progress of a femtosecond fiber timing distribution system for the Linac Coherent Light Source (LCLS) [1-3] at SLAC to enable the machine diagnostic at the 10 fs level. The LCLS at the SLAC is the world's first hard x-ray free-electron laser (XFEL) with unprecedented peak brightness and pulse duration [1-3]. The time-resolved optical/x-ray pump-probe experiments at this facility open the era of exploring the ultrafast dynamics of atoms, molecules, proteins, and condensed matter [4-6]. However, the temporal resolution of current experiments is limited by the timing jitter between the optical and x-ray pulses [7, 8]. Recently, sub-25 fs root mean squared (rms) jitter is achieved from an x-ray/optical cross-correlator at the LCLS [9], and external seeding is expected to reduce the intrinsic timing jitter [10, 11], which would enable full synchronization of the optical and x-ray pulses with sub-10 fs precision. For such a technique, tight synchronization between seed and pump lasers needs to be implemented [12-16]. Preliminary test results of the major components for a 4 link system will be presented. Currently, the system is geared towards diagnostics to study the various sources of jitter at the LCLS.

INTRODUCTION

The emergence of few fs x-ray pulses generated from state-of-the-art XFELs [2, 3] has enabled the study of ultrafast phenomenon using optical/x-ray pump-probe techniques. In these time-resolved experiments, timing synchronization of x-ray and optical pulses at the precision of or below 10 fs is required, which is beyond the performance of traditional rf-based synchronization systems on the order of 100 fs rms [7]. Although it has been demonstrated recently that sub-10 fs precision can be reached by the x-ray optical cross-correlator and post-analysis [17], such characterization technique requires substantial x-ray pulse energy and it is not practical to install such device at every time-resolved experiment at the LCLS. In order to provide sub-10 fs precision, a pulsed laser timing synchronization and distribution system is adopted. The optical pulse train fulfils two tasks: first, it serves as the means for stabilizing the group delay of the pulses in the fiber link to a multiple of the repetition time of the pulses with femtosecond precision. Secondly, a fraction of the pulse train is coupled out from each end of the fiber link and is used to synchronize microwave or optical sub-systems to the reference rf. The optical-optical and optical-microwave synchronization modules used in the system are all based on balanced detection techniques which are with high dynamic range free of AM-to-PM noise conversion [12-16]. As a result, such systems allow for more accurate timing control in time-resolved experiments at the LCLS. On the other hand, it could serve as an alternative timing diagnostic tool when neither x-ray pulse nor x-ray/optical cross-correlator is available. In this paper, progress towards implementation of the pulsed laser timing system and preliminary experimental results are presented.

* This work is partially supported by the DOE STTR Award DE-SC0004702.

SYSTEM DESIGN AND EXPERIMENT

There are two major challenges in synchronizing the x-ray and optical pulses to the 10-fs level: one is to preserve the timing signal at the experimental hutches hundreds of meters downstream the accelerator RF pickup location [1]; the other is to precisely synchronize the Ti:sapphire lasers and transport the beam to the interaction point of the experiment. The proposed system layout for LCLS is shown in Fig. 1. We use a low-noise Er-doped fiber laser as the optical master clock (OMO). Since the undulator tunnel is usually inaccessible during beam time, the OMO is placed in the laser hall and its pulse train is sent to the end of the undulator tunnel through hundreds meters of timing-stabilized fiber-link (FLS) [12]. The timing signal encoded on the laser pulse train is compared against the accelerator RF picked up by the phase cavity using a balanced-optical microwave phase detector (BOM-PD) [13]. The baseband error signal is fed back to the OMO

ISBN 978-3-95450-126-7

via a copper cable to stabilize the OMO. Inside the laser hall, the Ti:sapphire oscillator seeding the amplifier is synchronized to the OMO by a two-color balanced optical cross-correlator (TC-BOC) [14]. Two additional TC-BOCs will be used to characterize the timing drifts of amplified pulses at the amplifier output as well as the point of interaction. To prevent interruption of LCLS operation, currently the system is being evaluated in the research laser laboratory of the LCLS; In the meantime, we are also planning to work on the system implementation during shutdowns of the LCLS. During the preliminary test, we used one local oscillator (Wenzel) at 476 MHz (6th subharmonic of 2856 MHz) as the radio-frequency master oscillator (RMO), instead of the actual accelerator RF from the phase cavity [1]. The FLS, BOM-PD, and TC-BOC are all commercial products from the idestaQE, LLC.

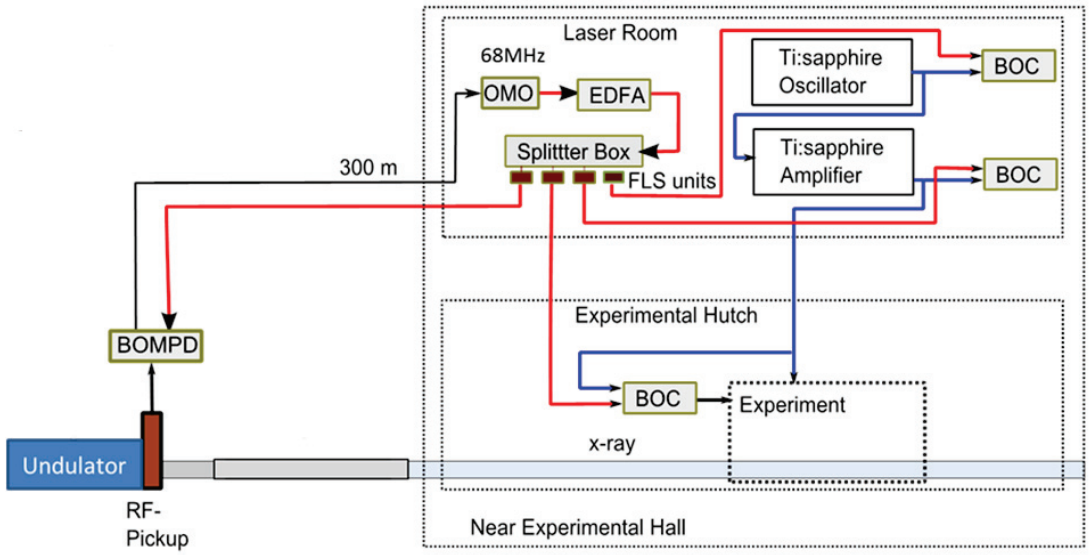

Figure 1: The system design. OMO, optical master oscillator; EDFA, Er-doped fiber amplifier; BOMPD, balanced-optical-microwave phase detector; BOC, (two-color) balanced optical cross-correlator; FLS, fiber link system.

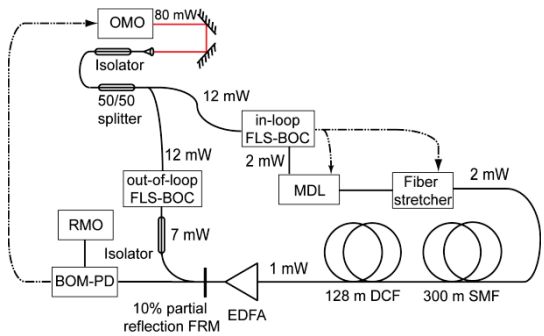

Figure 2: The fiber link system scheme and power distribution. OMO, optical master oscillator; RMO, radio frequency master oscillator; BOM-PD, balanced-optical-microwave phase detector; FLS-BOC, fiber link system balanced optical cross-correlator; MDL, motorized delay line; SMF, single mode fiber; DCF, dispersion compensating fiber; EDFA, Er-doped fiber amplifier; FRM, Faraday rotating mirror. The dashed lines stand for the feedback.

Fig. 2 shows the experimental setup for testing remote RMO-OMO synchronization with a FLS and a BOM-PD. The OMO is a commercial 68MHz Er-doped fiber laser which delivers nearly transform-limited pulses with output pulse duration of ~200fs. The light is first coupled into free-space and then back into a polarization maintaining (PM) single-mode fiber for easy optimization of input power to the FLS. The pulses from the OMO are split into two arms with a 50/50 splitter; one arm goes into the in-loop FLS-BOC for detecting the timing drifts from the fiber link and uses it as an error signal for timing control; the other arm goes into another FLS-BOC to measure the out-of-loop residual timing jitter and drifts. The fast and slow timing errors are compensated by a PM piezo fiber stretcher and a motorized delay line, respectively to compensate slow timing drifts. Each FLS-BOC has a 4 mm periodically poled potassium titanyl phosphate (PPKTP) crystal for generating efficient sum frequency generation (SFG) light using type II phase-matching. The SFG is generated by the pulses directly from the OMO (reference arm) and the pulses that travel back and forth through the fiber link (link arm). The sensitivity is calibrated by the s-curve that maps the timing jitter to voltage [12, 15, 16]. The fiber link consists 300 m single mode fiber (SMF) (β_2=-23 fs^2/mm) and 128 m dispersion compensating fiber (β_2=40 to 60 fs^2/mm). The net group velocity dispersion of the fiber link is close to zero; the difference in mode field diameter between standard single-mode fiber and dispersion compensating fiber results in 3 dB power loss (Fig. 2). The pulse is amplified by an EDFA at the end of the link to recover the power loss after the round-trip. 10% of the light is

ISBN 978-3-95450-126-7

reflected by a Faraday reflecting mirror (FRM) to the FLS-BOC; 90% of the power goes into the out-of-loop FLS-BOC for experiments, or the BOM-PD for synchronization.

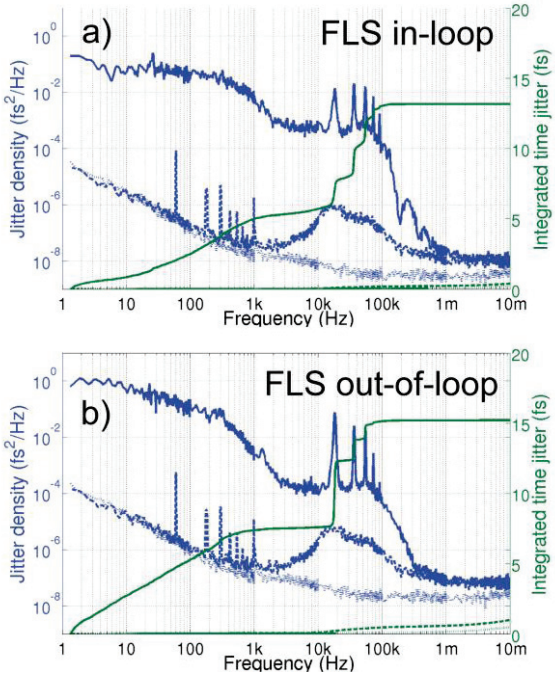

Figure 3: The fiber link system performance: (a) in-loop and (b) out-of-loop phase noise measured by the FLS-BOC with a vector signal analyzer (VSA). The solid, dashed, and dotted traces are the measurement, detector background, and VSA background separately; the blue traces are the phase noise density measurements, and the green traces are the integrated timing jitters of the noise densities.

In order to avoid the nonlinearity, and to achieve near transform-limited pulses in both in-loop and out-of-loop FLS-BOCs; the input power to the fiber link is optimized to be 2 mW. Fig. 3 shows the power spectral density of in-loop and out-of-loop phase noise measured with a vector signal analyzer (HP 89410A), which has very similar distribution. The timing jitter integrated from 1-10kHz is 6 fs and 7 fs in the in-loop and out-of-loop measurement, respectively. The spectral peaks at 18 kHz and its harmonics, which match the resonant frequency of the piezo stretcher, also contribute to about 8 fs in both measurements. However, we believe these peaks are just artifacts excited by the interference between SFG and second harmonic generation (SHG) from the pulses of the reference arm. We have verified with a CCD camera that a small amount of SHG was generated in the background which modulated the cross-correlation traces at a period of the fundamental wavelength. The SHG could result from the misalignment of the PPKTP crystal due to a non-ideal crystal mount design. We have designed new mounts which will be tested soon.

Once the fiber-link is stabilized, the OMO is then synchronized to the RMO using the BOM-PD. The BOM-PD takes the seventh harmonic of the repetition rate of the optical pulse train and compares it against the 476 MHz RMO, resulting in a timing sensitivity up to 8 μV/fs, as shown in Fig. 4. The error signal from the BOM-PD is sent to a proportional integrator controller and then amplified by a high voltage amplifier. The output is used to drive the piezo mirror inside the OMO in order to change the cavity length and thus the timing of the optical pulse train.

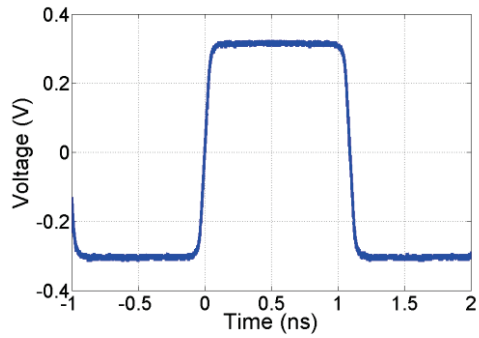

Figure 4: The sensitivity of the BOM-PD.

Fig. 5 shows the phase noise density for the remote RMO and the synchronized OMO. It can be seen that the locked OMO follows the phase noise of RMO at low frequencies and preserves its noise at high frequencies. Currently, the sensitivity of the BOM-PD is reduced to about 3 μV/fs since the output power of the fiber link is low, which limits the performance of the synchronization. We are currently building a new EDFA, which will provide more power to the BOM-PD and therefore, higher sensitivity for better synchronization.

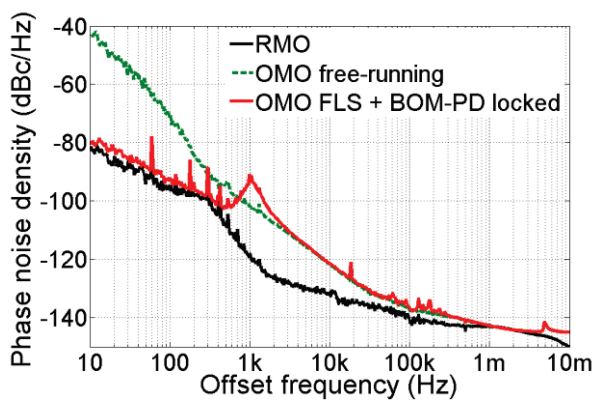

Figure 5: Phase noise densities (measured with a Agilent signal source analyzer (SSA) at 2856 MHz) of the OMO locked to the remote RMO by the stabilized fiber link system and BOM-PD. The green trace is the phase noise of the free-running OMO; the red trace is the phase noise of the locked OMO; the black trace is the phase noise of the reference RMO.

ISBN 978-3-95450-126-7

Locking of the Ti:sapphire laser to the OMO is very important for time-resolved optical/x-ray pump probe experiments; after synchronizing the OMO to the RMO, we locked the Ti:sapphire laser to the OMO by a TC-BOC, which acts as an optical mixer and uses the balanced detection to suppress against AM-to-PM conversion [14]. The experimental schematic is shown in Fig. 6: both TC-BOCs have 7 mW input power from the OMO and 100 mW power from the Ti:sapphire oscillator. The 1550 nm and the 800 nm light is mixed in a barium borate (BBO) crystal to produce the forward and backward cross-correlation traces. The difference between two time-delayed cross-correlations produces the s-curve which maps the timing jitter into a voltage signal [14]. The in-loop and out-of-loop TC-BOC uses a 2-mm and a 1-mm BBO crystal with a timing sensitivity as high as 14 mV/fs (as shown in Fig 7(a)) and 0.2 mV/fs at the centre of the s-curve, respectively. Fig. 7(b) shows the jitter density obtained with the out-of-loop TC-BOC, which gives about 20 fs rms integrated jitter from 1 Hz to 10 MHz. It should be emphasized that what is shown here are first results which have not been optimized. For example, the out-of-loop TC-BOC does not have enough sensitivity mainly due to the low efficiency of the SFG with a 1-mm BBO crystal; we expect larger sensitivity by using a 2-mm BBO crystal. Also, we need to confirm that the laser was locked to the correct locking point since there are more than one zero-crossing points on the s-curve as shown in Fig 7(a).

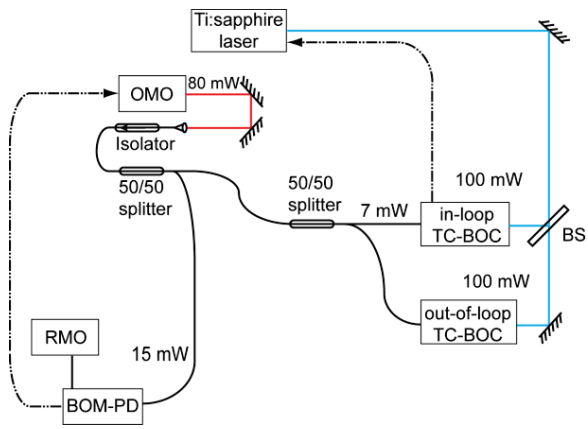

Figure 6: The TC-BOC experimental scheme. OMO, optical master oscillator; RMO, radio master oscillator; BOM-PD, balanced optical microwave phase detector; BS, beam splitter; TC-BOC, two-color balanced optical cross-correlator. The dashed lines indicate electronic feedback paths.

SUMMARY AND CONCLUSION

In summary, progress towards the implementation of a 10-fs pulsed laser timing system at LCLS and preliminary experimental results are presented. Two major experiments including synchronizing the OMO to the remote RMO using a BOM-PD and a FLS as well as optical-optical synchronization of the Ti:sapphire laser and the OMO with a TC-BOC have been demonstrated. We are currently working on improving the system performance and to perform several long-term system tests. In the meantime, we are also planning the implementation of the system at the LCLS in the next few months.

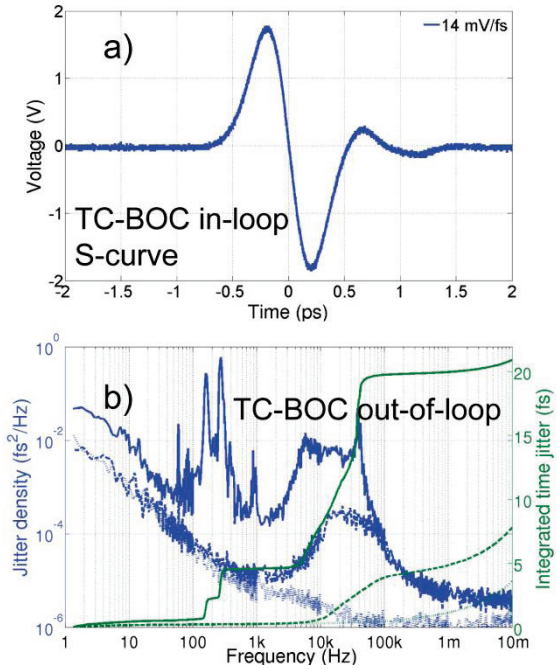

Figure 7: The TC-BOC experiment. a) the in-loop S-curve; b) the out-of-loop timing jitter spectral density and its integrated timing jitter. The colors and shapes of the traces have the same interpretation as in Fig. 3.

ACKNOWLEDGEMENT

We would like to thank Steve Edstrom for his help on improving the stability of the lab environment. This work is partially supported by the DOE STTR Award DE-SC0004702.

REFERENCES

[1] P. Emma et al., "First lasing and operation of an ångstrom-wavelength free-electron laser," Nat. Photonics 4, 641-647 (2010).

[2] Y. Ding et al., "Measurements and Simulations of Ultralow Emittance and Ultralow Emittance and Ultrashort Electron Beams in the Linac Coherent Light Source," Phys. Rev. Lett. 102, 254801 (2009).

[3] Y. Ding et al., "Femtosecond X-Ray Pulse Characterization in Free-Electron Lasers Using a Cross-Correlation Technique," Phys. Rev. Lett. 109, 254802 (2012).

[4] A. H. Zewail, "Femtochemistry: Atomic-Scale Dynamics of the Chemical Bond," J. Phys. Chem. A, 104, 5660 (2000).

[5] J. P. Cryan et al., "Auger Electron Angular Distribution of Double Core-Hole States in the

ISBN 978-3-95450-126-7

Molecular Reference Frame," Phys. Rev. Lett. 105, 083004 (2010).
[6] V. S. Petrović et al., "Transient X-Ray Fragmentation: Probing a Prototypical Photoinduced Ring Opening," Phys. Rev. Lett., 108, 253006 (2012).
[7] J. M. Glownia et al., "Time-resolved pump-probe experiments at the LCLS," Opt. Express, 18, 17620 (2010).
[8] F. Tavella et al., "Few-femtosecond timing at fourth-generation X-ray light sources," Nat. Photonics 5, 162- 165 (2011).
[9] M. R. Biont et al., "Spectral encoding of x-ray/optical relative delay," Opt. Express, 19, 21855-21865 (2011).
[10] G. Stupakov, "Using the Beam-Echo Effect for Generation of Short-Wavelength Radiation," Phys. Rev. Lett. , 102, 074801 (2009).
[11] D. Xiang et al., "Evidence of High Harmonics from Echo-Enabled Harmonic Generation for Seeding X-Ray Free Electron Lasers," Phys. Rev. Lett. , 108, 024802 (2012).
[12] J. Kim et al., "Long-term femtosecond timing link stabilization using a single-crystal balanced cross correlator," Opt. Lett., 32, 1044 (2007).
[13] J. Kim et al., "Balanced optical-microwave phase detectors for optoelectronic phase-locked loops," Opt. Letters, 31, 3659 (2006).
[14] J. Kim et al., "Attosecond-resolution timing jitter characterization of free-running mode-locked lasers," Opt. Lett., 32, 3519 (2007).
[15] J. Kim et al., "Drift-free femtosecond timing synchronization of remote optical and microwave sources," Nat. Photonics 2, 733-736 (2008).
[16] S. Schulz et al., "An Optical Cross-Correlation Scheme to Synchronize Distributed Laser Systems at FLASH," 11th European Particle Accelerator Conference, Genoa, Italy, 23 - 27 Jun 2008, pp.THPC160.
[17] M. Harmand, et al., "Achieving few-femtosecond time-sorting at hard X-ray free-electron lasers," Nat. Photonics 7, 215–218 (2013).

ISBN 978-3-95450-126-7